DEPENDENCE OF GEOMETRICAL CONFIGURATION ON MECHANICAL BEHAVIOUR OF GFRP COMPOSITE SANDWICHES

Antonino Valenza[1], Vincenzo Fiore[1] and Luigi Calabrese[2]

[1] Dept. of Ingegneria Chimica dei Processi e dei Materiali, University of Palermo, 90128 Palermo, Italy
[2] Dept. of Chimica Industriale e Ingegneria dei Materiali, University of Messina, 98166 Messina, Italy

ABSTRACT

Aim of this research work is to find the dependence of geometrical configuration on failure mechanism of composite sandwiches subjected to three point bending test.
All tested structures have been realized at room temperature, with a single lamination, by vacuum bagging technique. These sandwiches are made up of two skin of E-glass/epoxy composite and closed-cell PVC foam cores with a density of 60 Kg/m^3. Experimental tests have been carried out at varying skin thickness (t) and span length between support (l) with the purpose to show the dependence of mechanical behaviour on these geometric parameters. From experimental results a failure map in the plane t - l has been created identifying three regions of typical failure modes of the sandwiches.

1. INTRODUCTION

When sandwich composites are subjected to three point bending, several failure mechanisms may occur: a failure mechanism will be shown when its breaking load results smaller in comparison of those ones of competitive mechanisms. In literature five main failure mechanisms have been identified: skin compressive/tensile failure, core shear failure, skin wrinkling, indentation and delamination, i.e skin-core debonding [1].
Consider a sandwich beam (Figure 1) with skins of equal thickness subjected to a bending moment M and shear force V.

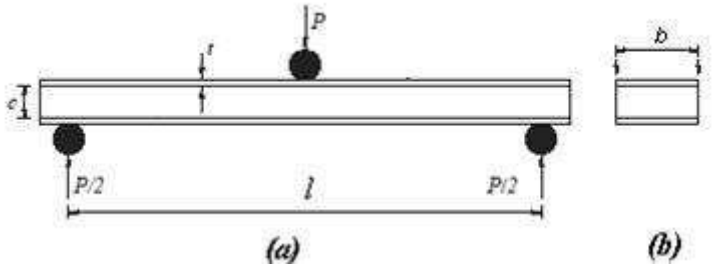

Figure 1: Experimental Schematic configurations of the foam core composite sandwich beam: (a) loading configuration and (b) cross section

For relatively thin skins and relatively low core stiffness, the bending moment is mainly taken up by the facings, while the shear stress is mainly taken up by the core.
The compressive or tensile skin stress σ_f, is [2]:

$$\sigma_f = \frac{M}{b \cdot t \cdot (t+c)} \cong \frac{M}{b \cdot t \cdot c} \qquad (1)$$

Since maximum bending moment is given by:

$$M = \frac{P \cdot l}{4} \qquad (2)$$

the compressive or tensile skin breaking load is:

$$P_f = \frac{4 \cdot b \cdot t \cdot (t+c) \cdot \sigma_f}{l} \approx \frac{4 \cdot b \cdot t \cdot c \cdot \sigma_f}{l} \qquad (3)$$

The shear stress τ_c in the core is:

$$\tau_c = \frac{V}{b \cdot (t+c)} \approx \frac{V}{b \cdot c} \qquad (4)$$

Since shear is given by:

$$V = \frac{P}{2} \qquad (5)$$

the core shear skin breaking load is [3,4]:

$$P_{CS} = 2 \cdot b \cdot (t+c) \cdot \tau_C \approx 2 \cdot b \cdot c \cdot \tau_C \qquad (6)$$

Skin wrinkling is defined as a localized short-wave length buckling of compression skin. It must be viewed as buckling of the compression facing supported on one side by the core. The value of the fracture load is given from the following expression [5]:

$$P_W = \frac{4 \cdot b \cdot t \cdot c}{l} \cdot 3 \cdot \left[\frac{E_f \cdot E_C^2}{12 \cdot (3 - \nu_C)^2 \cdot (1 + \nu_C)^2} \right] \qquad (7)$$

Indentation of the core occurs at concentrated load, such as fittings, corners, or joints. Practically they can be avoided by applying the load over a sufficiently large area [3]. This area can be estimated from [6]:

$$A = \frac{P}{\sigma_C} \qquad (8)$$

Where σc is the compressive strength of the core material.

Triantafillou and Gibson [6] assumed that the indentation load is dictated by plastic yield of the core but the contribution from the skins is ignored. This approximation is valid for the case of thin skins but fails for practical sandwich beams.

Ashby et al. [7] have considered the indentation strength due to the combined plastic collapse of the face sheets and core. They treat both the skins and the core as rigid, ideally plastic solids, with the core undergoing compressive yield and the skins forming plastic hinges. This model was confirmed by a series of experiments and detailed numerical simulations on metallic foam cores and aluminium alloy skins [8,9].

In another work [10] it is shown experimentally and by finite element analysis that the indentation load is set by elastic deformation of the faces and compressive yield of the core. These failure mechanisms are called ductile indentation and elastic indentation respectively [11].

In the case of failures like delamination and skin-core debonding it is very difficult to perform a theoretical strength prediction analysis from the knowledge of the mechanical characteristics of the skin and the core.

2. EXPERIMENTS

Four type of symmetrical sandwiches at room temperature by vacuum bagging technique are realised. Structures prepared consist of a common PVC foam core and GFRP skins with one (named M1), two (M2), three (M3) and four layer (M4) respectively.

The core is constituted by a “closed cell” PVC foam (Herex® C 70.55 from Alcan composites) having density of 60 Kg/m3 and thickness c equal to 5 mm.

The sandwich beam skins were realized with E-glass mat (randomly oriented fibres, with density of 300 g/m^2) and a SR 8100 epoxy resin combined with the hardener SR 8822, both supplied by Sicomin, used as matrix.
Experimental tests have been carried out by using a Universal Testing Machine (UTM) mod. 3365 by Instron, equipped with a load cell of 5 KN, with a speed of 1 mm/min.
For every sandwich, three point flexural tests were carried out on rectangular samples with width b = 15 mm placing span distance l equal to 40, 50, 60, 80, 100, 120, 140, 160, 180 and 200 mm. For each condition, five samples have been tested. Average values of skin thickness t are reported in Table 1 .

l [mm]	M1	M2	M3	M4
30	0,326 ± 0,023	1,128 ± 0,033	1,655 ± 0,064	2,517 ± 0,076
40	0,365 ± 0,011	1,014 ± 0,078	1,802 ± 0,030	2,284 ± 0,126
50	0,362 ± 0,018	0,905 ± 0,035	1,823 ± 0,064	2,419 ± 0,088
60	0,358 ± 0,041	0,930 ± 0,030	1,739 ± 0,024	2,316 ± 0,039
80	0,341 ± 0,024	1,107 ± 0,058	1,680 ± 0,014	2,280 ± 0,065
100	0,376 ± 0,026	0,975 ± 0,031	1,776 ± 0,046	2,399 ± 0,049
120	0,367 ± 0,033	1,107 ± 0,044	1,471 ± 0,059	2,472 ± 0,102
140	0,324 ± 0,041	1,037 ± 0,032	1,547 ± 0,013	2,444 ± 0,078
160	0,351 ± 0,038	1,018 ± 0,035	1,559 ± 0,035	2,268 ± 0,044
180	0,257 ± 0,016	0,849 ± 0,056	1,545 ± 0,037	2,395 ± 0,067
200	0,277 ± 0,031	1,045 ± 0,138	1,607 ± 0,029	2,401 ± 0,089

Table 1. Average values of skin thickness for each condition investigated

4. EXPERIMENTAL RESULTS

The experimental mechanical tests show that three failure mechanism have been take place: two different indentation failures (called type I and type II) and tensile failure of the lower skin.
In Figure 3 are showed three typical and representative load/width ratio versus displacement curves, each one relative to a failure mechanism experimental obtained.

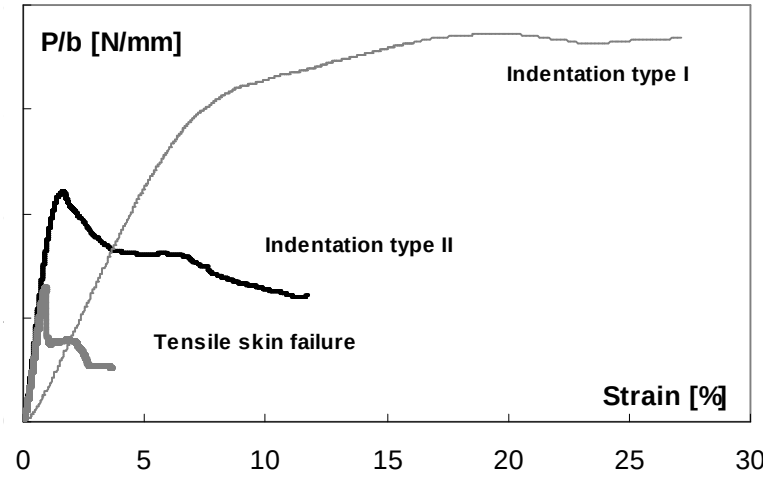

Figure 2. Flexural test graphs

All curve show an initial linear trend with different slope. In particular samples fractured for tensile skin failure and indentation type II have similar slope while the other one shows smaller slope.
Indentation type II and tensile skin failure occur, the first at higher loads than the second one, with a significant loss of the load-carrying capability.
In Figure 3 is shown the first type of indentation. From this picture it is possible to notice that the core yields without skin failure under localized load. This is a non catastrophic failure mechanism due to progressive collapse of the cell structure of the foam.
In the load application point the densification of PVC foam takes place due to the initial buckling fracture of the cell walls of PVC core; this brings to a strong local width reduction of the sandwich. At high deflection the lower skin fracture appears.

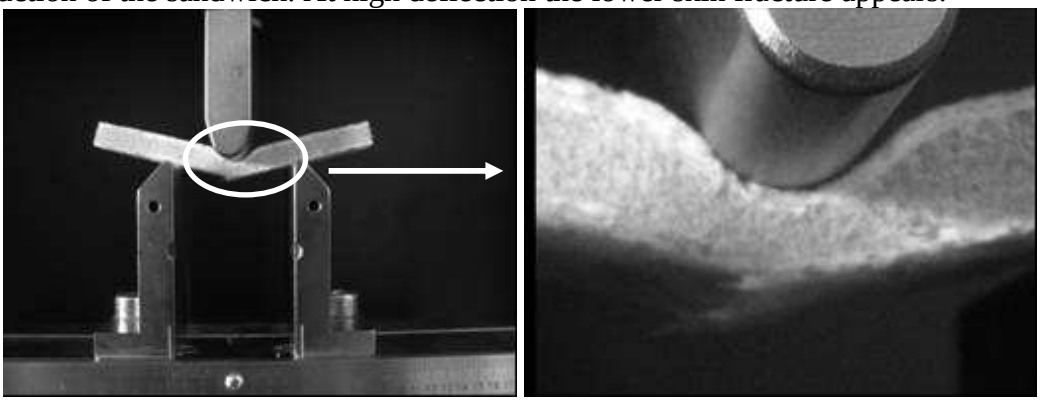

Figure 3. Indentation type I

In the case of indentation type II (Figure 4) the upper skin is heavy deformed due to the local applied load. This condition influence the failure mechanism that occur in this region due to the collapse of the upper skin. After that the crack propagates across the core reaching occasionally the lower skin. In all cases no delamination was evidenced at the skin-core interface.

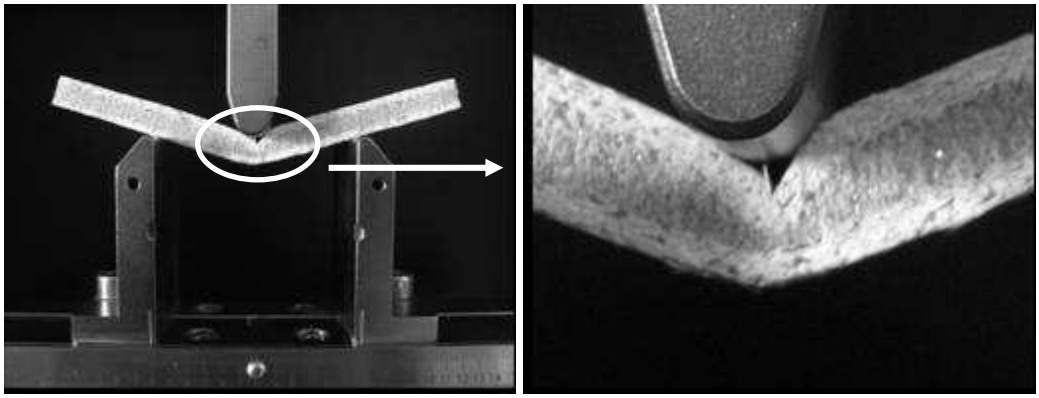

Figure 4. Indentation type II

In the case of tensile skin failure (Figure 5) the crack start in the lower skin. It propagate usually at the skin-core interface before to propagate across the core. The crack finish at the upper skin-core interface.

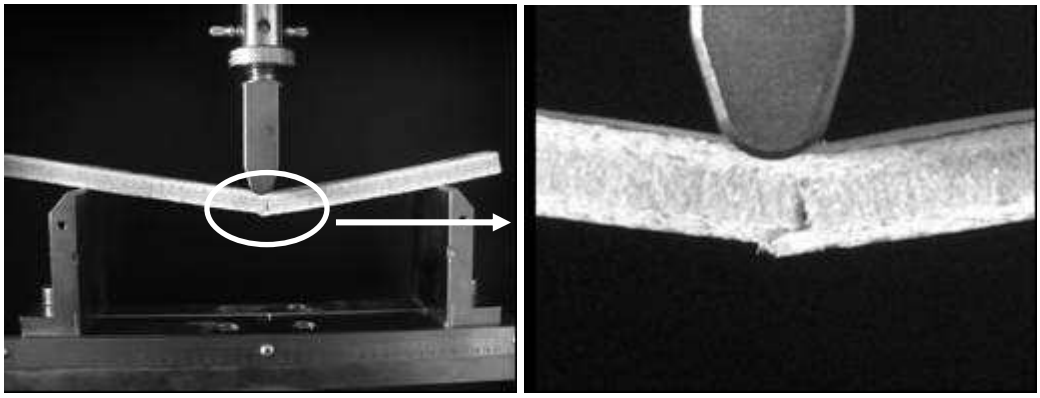

Figure 5. Tensile skin failure

4.1 Flexural tests at varying the parameter "l"

The flexural tests results obtained at varying distance span l for a fixed value of skin thickness t are reported in Figure 6.

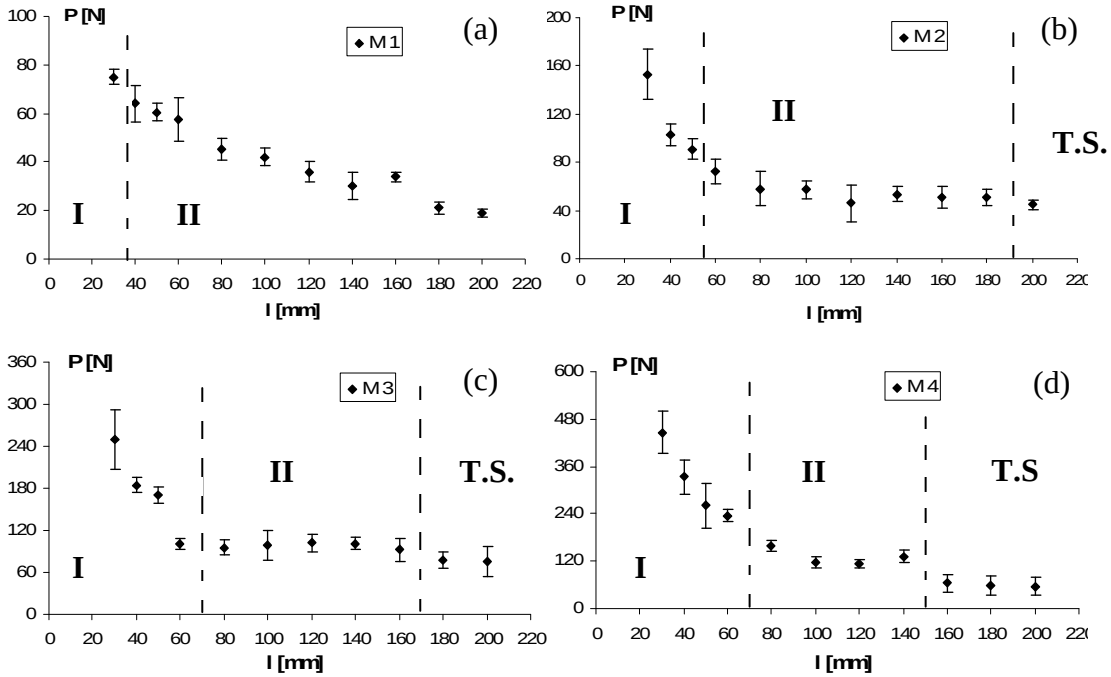

Figure 6. Maximum load at varying "l" for sample M1 (a), M2 (b), M3 (c) and M4 (d)

From Figure 6 (a), it's possible to observe that samples M1 (characterized by one layer skin) show only indentation type II fractures except for the sample with l = 30 mm where the failure occurs for indentation type I. With increasing distance span l a reduction of the maximum load P is obtained

As shown in Table 6 samples M2 (characterized by two layer skin) show indentation I failures for l inferior to 60 mm and indentation type II for the other samples except for the sample with l = 200 mm where tensile skin failure occurs. The maximum load P decreases with increasing l for the samples that show indentation I instead it remains constant in the range of indentation II (Figure 6 (b)).

Samples M3 (three layer skin) show indentation type II failures for l between 80 mm and 160 mm, indentation type I for l less than 80 mm and tensile skin failures for l greater than 160 mm. In the range of indentation I, the maximum load P decreases with increasing l. For higher values of l, P assumes constant values for each failure

mechanisms (an higher value for indentation II than tensile skin) as shown in Figure 6 (c).
Samples M4 (four layer skin) show indentation II failures for l between 80 mm and 140 mm, indentation I for l less than 80 mm and tensile skin for l greater than 140 mm. In the ranges of all failure mechanisms obtained, the maximum load P presents similar trends like those ones shown for samples M3 as shown in Figure 6 (d).
In the cases of samples M3 and M4 (compared with samples M1 and M2) the range of indentation type I becomes larger and failure by tensile skin becomes prevalent mechanism in a larger area for high values of l with the consequence that range of indentation II become smaller.

4.2 Failure map

From the experiments it has been found how geometrical parameters influence the fracture mode of the sandwiches. These results can be better evidenced creating a failure map, plotting the failure mechanisms as a function of thickness and length. In this map it is possible to notice the existence of three regions in which one of the failure mechanisms experimental obtained is dominant.

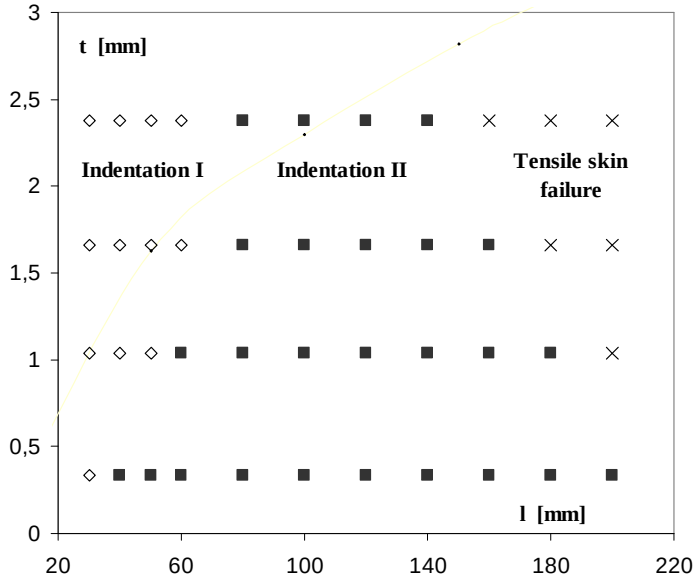

Figure 7. Failure map

Particularly for high t and l values tensile skin failure occurs. At decreasing of l two transition are observed:

- Between tensile skin and indentation type II for l values comprised between 140 mm and 180 mm
- Between indentation II and indentation I for l values comprised between 30 mm and 60 mm

At decreasing of t a transition is observed between tensile skin failure and indentation II. This transition occurs for t values comprised between 0,3 mm and 1,7 mm.
For intermediate l values failure mechanism predominant is indentation type II (any value of t). Decreasing l a transition between indentation II and I is observed for l values increasing with t.
A failure mechanism will take place when its breaking load results smaller in comparison of those ones of other competitive mechanisms. As shown in Figure 7, indentation mechanisms are usually obtained whereas tensile skin failure happens in a limited area of the map (with limited geometrical conditions). This phenomenon can be explained by theoretical consideration. Indentation breaking loads are a function of core

mechanical properties instead tensile skin breaking loads are independent from these properties as seen in equation (3). Due to low mechanical properties of PVC foam core used in present work, indentations breaking loads result lower than tensile failure one in most of the tests.

5. CONCLUSIONS

In this work, the static failure modes of E-glass/epoxy composite and closed-cell PVC foam cores sandwich were investigated experimentally by three point flexural tests. The study was focused on the dependence of geometrical parameters, such as skin thickness (t) and span length between support (l), in the failure mechanism.

Four type of symmetrical sandwiches with different number of layers (and consequently different thickness) have been prepared and characterized by three point flexural tests varying span length, l (from 40 to 200 mm).

From experimental results a failure map in the plane t - l has been created identifying three regions of typical failure modes of the sandwiches.

A further our purpose is to develop in the future a theoretical model able to forecast the experimental failure mechanism. In this way predictive capacity of this model could be quite helpful in the sandwich structure design.

REFERENCES

1- Corigliano A.Z., Rizzi E. and Papa E., "Experimental characterization and numerical simulations of a syntactic-foam/glass-fibre composite sandwich". *Composite Science and Technology*, 2000;60:2169–80.
2- Konsta-Gdoutos, M.S., and Gdoutos, E.E., "The Effect of load and geometry on the failure modes of sandwich beams". *Applied Composite Materials*, 2005;12:165-176.
3- Zenkert D., "An introduction to sandwich construction". Sheffield, UK: Engineering Material Service; 1995
4- Plantema F., "Sandwich Construction". New York: Wiley; 1996
5- Allen H.G., "Analysis and design of structural sandwich panels". Pergamon, 1969.
6- Triantafillou T., Gibson L.J., "Failure mode maps for foam core sandwich beams". *Materials Science and Engineering*. 1987;95:37-53
7- Ashby M.F., Evans A.G., Fleck N.A., Gibson L.J., Hutchinson J.W., Wadley H.N.G., "Metal foams: a design guide". London: Butterworth, Heinemann; 2000
8- Chen C., Harte A.M., Fleck N., "The plastic collapse of sandwich beams with a metallic foam core". *International Journal of Mechanical Sciences*, 2001;43:1483–506.
9- McCormack T., Miller R., Kesler O., Gibson L., "Failure of sandwich beams with metallic foam cores". *International Journal of Solids and Structures*, 2001;38:4901–20.
10- Steeves C.A., Fleck N.A., "Collapse mechanisms of sandwich beams with composite faces and a foam core, loaded in three-point bending. Part II: experimental investigation and numerical modelling". *International Journal of Mechanical Sciences*, 2004;46:585–608.
11- Steeves C.A., Fleck N.A., "Material Selection in sandwich beam construction". *Scripta Materialia*, 2004;50:1335-1339
12- Gibson L.J., Ashby M.F., "Sandwich structures, Cellular solids: structure and properties". 2nd ed, Cambridge U.P., Cambridge; 1997.